

8-2016

High-sensitivity Mass Spectrometry for Probing Gene Translation in Single Embryonic Cells in the Early Frog (*Xenopus*) Embryo

Camille Lombard-Banek
George Washington University

Sally Ann Moody
George Washington University

Peter Nemes
George Washington University

Follow this and additional works at: https://hsrc.himmelfarb.gwu.edu/smhs_anatregbio_facpubs

 Part of the [Anatomy Commons](#), [Animals Commons](#), and the [Cell and Developmental Biology Commons](#)

APA Citation

Lombard-Banek, C., Moody, S. A., & Nemes, P. (2016). High-sensitivity Mass Spectrometry for Probing Gene Translation in Single Embryonic Cells in the Early Frog (*Xenopus*) Embryo. *Frontiers in Cell and Developmental Biology*, 4 (). <http://dx.doi.org/10.3389/fcell.2016.00100>

This Journal Article is brought to you for free and open access by the Anatomy and Regenerative Biology at Health Sciences Research Commons. It has been accepted for inclusion in Anatomy and Regenerative Biology Faculty Publications by an authorized administrator of Health Sciences Research Commons. For more information, please contact hsrc@gwu.edu.

High-sensitivity Mass Spectrometry for Probing Gene Translation in Single Embryonic Cells in the Early Frog (*Xenopus*) Embryo

Camille Lombard-Banek¹, Sally A. Moody², Peter Nemes^{1*}

¹Department of Chemistry, George Washington University, USA, ²Department of Anatomy and Regenerative Biology, George Washington University, USA

Submitted to Journal:
Frontiers in Cell and Developmental Biology

Specialty Section:
Molecular Medicine

ISSN:
2296-634X

Article type:
Methods Article

Received on:
01 Jun 2016

Accepted on:
29 Aug 2016

Provisional PDF published on:
29 Aug 2016

Frontiers website link:
www.frontiersin.org

Citation:
Lombard-banek C, Moody SA and Nemes P(2016) High-sensitivity Mass Spectrometry for Probing Gene Translation in Single Embryonic Cells in the Early Frog (*Xenopus*) Embryo. *Front. Cell Dev. Biol.* 4:100. doi:10.3389/fcell.2016.00100

Copyright statement:
© 2016 Lombard-banek, Moody and Nemes. This is an open-access article distributed under the terms of the [Creative Commons Attribution License \(CC BY\)](https://creativecommons.org/licenses/by/4.0/). The use, distribution and reproduction in other forums is permitted, provided the original author(s) or licensor are credited and that the original publication in this journal is cited, in accordance with accepted academic practice. No use, distribution or reproduction is permitted which does not comply with these terms.

Provisional

1 **High-sensitivity Mass Spectrometry for Probing Gene Translation in**
2 **Single Embryonic Cells in the Early Frog (*Xenopus*) Embryo**
3

4 Camille Lombard-Banek¹, Sally A. Moody², and Peter Nemes^{1*}
5

6 ¹Department of Chemistry and ²Department of Anatomy and Regenerative Biology

7 The George Washington University, Washington, DC 20052
8

9 *Correspondence to: Peter Nemes, 800 22nd Street, NW, Suite 4000, Washington, DC 20052,

10 USA; peter@gwu.edu, (Tel.) 202-994-5663
11

12 **Keywords:** Single-cell analysis, mass spectrometry, proteomics, cell differentiation, *Xenopus*

13 *laevis*

14 **Article Type:** Methods

15 **Abstract**

16 Direct measurement of protein expression with single-cell resolution promises to deepen the
17 understanding of the basic molecular processes during normal and impaired development. High-
18 resolution mass spectrometry provides detailed coverage of the proteomic composition of large
19 numbers of cells. Here we discuss recent mass spectrometry developments based on single-cell
20 capillary electrophoresis that extend discovery proteomics to sufficient sensitivity to enable the
21 measurement of proteins in single cells. The single-cell mass spectrometry system is used to
22 detect a large number of proteins in single embryonic cells of the 16-cell embryo of the South
23 African clawed frog (*Xenopus laevis*) that give rise to distinct tissue types. Single-cell
24 measurements of protein expression provide complementary information on gene transcription
25 during early development of the vertebrate embryo, raising a potential to understand how
26 differential gene expression coordinates normal cell heterogeneity during development.

27 **Introduction**

28 Single-cell analysis technologies are essential to understanding cell heterogeneity during
29 normal development and disease. Characterization of the genomes and their expression at the
30 levels of the transcriptome, proteome, and metabolome provides a molecular window into basic
31 cell processes. Single-cell measurements complement traditional cell population-averaging
32 approaches by enabling studies at the level of the building blocks of life, where many critical
33 processes unfold (Raj and van Oudenaarden, 2008; Altschuler and Wu, 2010; Singh et al., 2010;
34 Zenobi, 2013). For example, by studying individual cells, it is possible to ask how cells give rise
35 to all the different types of tissues in the body (stem cells) and specialize for defense (immune
36 cells), communication (neurons), and support (glia). This information in turn lays the foundation
37 to developing diagnosis and treatments for addressing pressing health concerns, such as
38 emergence of drug resistant bacteria, onset and development of neurodegeneration and cancer, as
39 well as infections.

40 Single-cell investigations take advantage of rapid developments in technology to obtain new
41 insights into systems cell biology. With more than million-fold amplification of DNA and RNA
42 and the commercialization of high throughput DNA and RNA sequencing, it is now possible to
43 query cell-to-cell differences (Kolisko et al., 2014; Mitra et al., 2014), including but not limited
44 to chromosomal mosaicism in tissues (Vijg, 2014; Gajecka, 2016) and embryonic somatic cells
45 (Liang et al., 2008; Jacobs et al., 2014), establishment of cell heterogeneity in the nervous system
46 (McConnell et al., 2013), and mutations during disease states (Junker and van Oudenaarden,
47 2015; Kanter and Kalisky, 2015). How gene expression translates into the functionally important
48 proteins and how they then feed back to modulate gene expression is essential to systems cell
49 biology. Multiple reports report differences between transcription and translation (Vogel and

50 Marcotte, 2012; Smits et al., 2014; Peshkin et al., 2015), and transcription is known to be
51 controlled by translational factors during development (Radford et al., 2008); therefore,
52 characterization of the proteome is critical to understanding cell heterogeneity. Translational cell
53 heterogeneity has traditionally been measured by immunohistochemistry and Western blot
54 analyses. Protein-targeted assays have recently gained substantial throughput by the
55 development of mass cytometry (CyTOF), which uses inductively coupled plasma and mass
56 spectrometry (MS) to simultaneously quantify ~35 different proteins tagged with rare earth
57 elements in thousands of cells. This level of multidimensionality has promoted applications in
58 cell differentiation during erythropoiesis (Bendall et al., 2011), and was recently coupled to
59 laser-ablation to spatially survey cell heterogeneity in the tumor environment (Giesen et al.,
60 2014).

61 Cell heterogeneity has particular significance during embryonic development. Over four
62 decades of innovative embryological manipulations combined with gene-by-gene identifications
63 and functional characterizations in *Xenopus* have shown that molecular asymmetries in the
64 distribution of maternal mRNAs occur upon fertilization and lead to the formation of the three
65 primary germ layers and the germ line (King et al., 2005; Lindeman and Pelegri, 2010). Recent
66 approaches have defined the spatial and temporal changes of mRNAs, abundant proteins and
67 metabolites in the whole embryo (Flachsova et al., 2013; Wuhr et al., 2014; De Domenico et al.,
68 2015). However, very little is known about how these molecules change over time in individual
69 blastomere lineages as they acquire germ layer and body axis fates. In many animals, mRNAs
70 that are synthesized during oogenesis are sequestered to different cytoplasmic domains
71 (Davidson, 1990; Sullivan et al., 2001), which after fertilization then specify the germ cell
72 lineage (King et al., 2005; Haston and Reijo-Pera, 2007; Cuykendall and Houston, 2010) and

73 determine the anterior-posterior and dorsal-ventral axes of the embryo (Heasman, 2006b;
74 Kenyon, 2007; Ratnaparkhi and Courey, 2007; White and Heasman, 2008; Abrams and Mullins,
75 2009). For example, in *Xenopus* several mRNAs are localized to the animal pole region, which
76 later gives rise to the embryonic ectoderm and the nervous system (Grant et al., 2014), whereas
77 localization of VegT mRNA to the vegetal pole specifies endoderm formation (Xanthos et al.,
78 2001), and region-specific relocalization of the Wnt and Dsh maternal proteins govern the
79 dorsal-ventral patterning of the embryo (Heasman, 2006a; White and Heasman, 2008). However,
80 there is abundant evidence that in developing systems not all transcripts are translated into
81 proteins; therefore, analyses of the mRNAs may not reveal the activity state of the cell. In fact,
82 different animal blastomeres of the 16-cell *Xenopus* embryo that are transcriptionally silent can
83 have very different potentials to give rise to neural tissues (Gallagher et al., 1991; Hainski and
84 Moody, 1992; Yan and Moody, 2007), even though they appear to express common mRNAs
85 (Grant et al., 2014; Gaur et al., 2016).

86 High-resolution MS is the technology of choice for the analysis of the proteome (Aebersold
87 and Mann, 2003; Guerrera and Kleiner, 2005; Walther and Mann, 2010; Zhang et al., 2013).
88 Using millions of cells, contemporary MS enables the discovery (untargeted) characterization of
89 the encoded proteomes of various species in near complete coverage, as recently demonstrated
90 for the yeast (Hebert et al., 2014), mouse (Geiger et al., 2013), and human (Kuster, 2014;
91 Wilhelm et al., 2014). Recent whole-embryo analyses by MS revealed that transcriptomic events
92 are accompanied by gross proteomic and metabolic changes during the development of *Xenopus*
93 (Sindelka et al., 2010; Vastag et al., 2011; Flachsova et al., 2013; Shrestha et al., 2014; Sun et al.,
94 2014), raising the question whether these chemical changes are heterogeneous also between
95 individual cells of the embryo at different embryonic developmental stages. However, the

96 challenge has been to collect high-quality signal from the miniscule amounts of small molecules
97 contained within single blastomeres for analysis. Since different blastomeres in *Xenopus* are
98 fated to give rise to different tissues (Moody, 1987b; a; Moody and Kline, 1990), elucidating the
99 proteome in individual cells of the embryo holds a great potential to elevate our understanding of
100 the cellular physiology that regulates embryogenesis. For a deeper understanding of the
101 developmental processes that govern early embryonic processes, it would be transformative to
102 assay the ultimate indicator of gene expression downstream of transcription: the proteome.

103 To address this cell biology question, we and others have developed platforms to extend MS
104 to single cells (see reviews in References (Mellors et al., 2010; Rubakhin et al., 2011; Passarelli
105 and Ewing, 2013; Li et al., 2015)). For example, targeted proteins have been measured in
106 erythrocytes (Hofstadler et al., 1995; Valaskovic et al., 1996; Mellors et al., 2010). Discovery
107 MS has been used in the study of protein partitioning in the nucleus of the *Xenopus laevis* oocyte
108 (Wuhr et al., 2015). Recently, we have developed single-cell analysis workflows and custom-
109 built microanalytical capillary electrophoresis (CE) platforms for MS to enable the discovery
110 (untargeted) characterization of gene translation in single embryonic cells (blastomeres). Using
111 single-cell CE, we have measured hundreds–thousands of proteins in blastomeres giving rise to
112 distinct tissues in the frog (*Xenopus laevis*), such as neural, epidermal, and gut tissues (Moody,
113 1987a). We have also established quantitative approaches to compare gene translation between
114 these cell types. Quantification of ~150 different proteins between the blastomeres has captured
115 translational cell heterogeneity in the 16-cell vertebrate embryo (Lombard-Banek et al., 2016a).
116 These results complement known transcriptional cell differences in the embryo, but also provide
117 previously unknown details on how differential gene expression establishes cell heterogeneity
118 during early embryonic development.

119 In this contribution, we give an overview of the major steps of the single-cell CE-MS
120 workflow (**Figure 1**). Protocols are provided to isolate single cells, extract and process proteins,
121 and use the CE-MS platform to identify and quantify protein expression. Additional details on
122 technology development and validation are available elsewhere (Nemes et al., 2013; Onjiko et
123 al., 2015b; Lombard-Banek et al., 2016a; Lombard-Banek et al., 2016b). These protocols have
124 allowed us to study proteins (Lombard-Banek et al., 2016a; Lombard-Banek et al., 2016b) and
125 metabolites (Onjiko et al., 2015b; Onjiko et al., 2016) in single blastomeres in 8-, 16-, and 32-
126 cell *Xenopus laevis* embryos. Additionally, trouble-shooting advice (**Table 2**) is provided to
127 help others adopt single-cell MS toward the systems biology characterization of molecular
128 processes in cells and limited amounts of specimens.

129 **Materials and Equipment**

130 **1. Single Blastomere Dissection**

- 131 a. Fine sharp forceps (e.g., Dumont #5). One forceps should have a squared tip, while the
132 other should be sharpened to a fine tip.
- 133 b. Sterile Pasteur pipets
- 134 c. Hair loop: place a fine hair (~10 cm long) into a 6" Pasteur pipet to form a 2–3 mm loop
135 and secure it in place with melted paraffin. Sterilize the hair loop before usage by dipping
136 it in 70% methanol.
- 137 d. 0.6 mL centrifuge tubes
- 138 e. 60 mm and 90 mm Petri dishes
- 139 f. Incubator set to 14 °C

- 140 g. Dejellying solution: 2% cysteine hydrochloride in water, pH 8, prepared by adding 20 g
141 of crystalline cysteine hydrochloride into 1 L of distilled water. pH is adjusted to 8 by
142 adding 10 N NaOH drop-wise.
- 143 h. 100% Steinberg's solution (SS): Dissolve the following salts into 1 L of distilled water:
144 3.5064 g NaCl, 49.9 mg KCl, 99.9 mg MgSO₄, 55.8 mg Ca(NO₃)₂, 0.6302 g Tris-HCl,
145 and 80.0 mg Tris-base. Adjust the pH to 7.4. Autoclave and store in 14 °C incubator.
- 146 i. 50% Steinberg's solution: Dilute 50 mL of 100% SS with 50 mL of distilled water.
- 147 j. Dissection dish: add 2 g of agarose in 100 mL of 100% Steinberg's solution. Dissolve the
148 agarose by autoclaving. Once the bottle is cool enough to handle, pour the agarose
149 mixture to ~1 mm in thickness into 60 mm in diameter Petri dishes. Alternatively, the
150 agarose mixture can be stored at 4 °C, and reheated in a microwave before use. Dishes
151 should be stored wrapped in plastic at 4 °C to prevent dehydration of the agarose.
- 152 k. *Xenopus laevis* (adult male and female). Protocols related to the handling and
153 manipulation of animals must adhere to Institutional and/or Federal guidelines; the work
154 reported here was approved by the George Washington University Institutional Animal
155 Care and Use Committee (IACUC #A311).

156 **2. Protein Extraction, Enzymatic digestion and Quantification**

- 157 a. Refrigerated centrifuge (4 °C)
- 158 b. Heat blocks (2) set to 60 °C and 37 °C.
- 159 c. A -20 °C freezer
- 160 d. Sonication bath (e.g., Brandson CPX 2800)
- 161 e. A vacuum concentrator (e.g., CentriVap, LabConco)

- 162 f. Lysis buffer: for 1 mL of lysis buffer, mix 100 μ L of 10% sodium dodecyl sulfate (SDS),
163 100 μ L of 1.5 M NaCl, 20 μ L of 1 M Tris-HCl (pH 7.5), 10 μ L of 0.5 M EDTA, and 770
164 μ L of H₂O.
- 165 g. Enzymatic digestion solution, 50 mM ammonium bicarbonate: add 0.1976 g of
166 crystalline ammonium bicarbonate to HPLC grade water.
- 167 h. Dithiothreitol (1 M): Dissolve 0.1543 g of solid dithiothreitol into 1 mL of 50 mM
168 ammonium bicarbonate. Divide in 50–100 μ L aliquots and store at –20 °C for months.
- 169 i. Iodoacetamide (1 M): Dissolve 0.1850 g of crystalline iodoacetamide into 1 mL of 50
170 mM ammonium bicarbonate. Iodoacetamide is light sensitive and therefore should be
171 kept away from any light sources. It is suggested to make freshly before use, but storage
172 in 50–100 μ L aliquots at –20 °C is acceptable for up to 2 months. Aliquots are only for
173 single use, do not freeze-thaw.
- 174 j. Trypsin solution: dissolve a 20 μ g vial in 40 μ L of 1 mM HCl in water.
- 175 k. Tandem mass tags kit (e.g., TMT10plex, Thermo Scientific)

176 3. CE-ESI-MS Analysis

- 177 a. HPLC grade solvents and reagents: water, acetonitrile, methanol, formic acid, and acetic
178 acid.
- 179 b. Regulated high voltage power supplies (2) outputting up to 5 kV for maintaining the
180 electrospray (e.g., P350, Stanford Research Systems), and up to 30 kV for CE separation
181 (e.g., Bertan 230-30R, Spellman)
- 182 c. Separation capillary: 40/110 μ m (i.d./o.d.) bare fused silica capillary from Polymicro.
- 183 d. Sample solution: mix 500 μ L methanol with 500 μ L water and 0.5 μ L acetic acid.
- 184 e. Sheath solution: add 50 mL of methanol to 50 mL of water and 50 μ L of formic acid.

185 f. Background electrolyte: to prepare 50 mL, mix 12.5 mL of acetonitrile, and 1.887 mL of
186 formic acid with 35.613 mL of water.

187 g. High-resolution mass spectrometer (e.g., Orbitrap Fusion, Thermo).

188 **Procedures**

189 **1. Sample Preparation**

190 The goal of sample preparation is to extract proteins from single cells and process the
191 proteins for MS analysis. The workflow (**Fig. 1**) starts with the identification of blastomeres in
192 the embryo in reference to established cell fate maps (Moody, 1987a; Lee et al., 2012) and
193 differences in cell size and pigmentation. Cells are microdissected using sharp forceps and
194 collected into individual microcentrifuge tubes. **Figure 2** shows the dissection of the V11 cell.
195 Next, isolated blastomeres are lysed using chemical (detergent) and physical (ultrasonication)
196 methods, and their proteins are extracted. The proteins are processed via standard bottom-up
197 proteomics protocols (Zhang et al., 2013), whereby reduction, alkylation, and enzymatic
198 digestion are performed to convert proteins into peptides that are more readily analyzable by MS.

199 **Single Blastomere Dissection and Isolation**

200 As detailed protocols are available on the identification and dissection of blastomeres (Moody,
201 2012; Grant et al., 2013), only a brief summary of the major steps follows.

202 1/ Prepare consumables:

- 203 • 2% cysteine solution
- 204 • 100% Steinberg solution (SS)
- 205 • 50% Steinberg solution (SS)
- 206 • Sterile Pasteur pipet

- 207 • Petri dish filled with 2% agarose (w/v in 100% SS)
 - 208 • Sharp forceps
 - 209 • Hair loop
 - 210 • 0.6 mL microcentrifuge tubes
- 211 2/ Remove jelly coats that naturally surround the embryos:
- 212 a. Add 4× volume of the cysteine solution to the embryos (**Table 1**) and gently swirl the
 - 213 solution for ~4 min.
 - 214 b. Once the embryos are free of the jelly coat, immediately wash them with 100% SS
 - 215 (**Table 1**) 4 times for 2 min each.
 - 216 c. Transfer the embryos to a clean Petri dish filled with 100% SS and store them at 14–20
 - 217 °C in an incubator.
- 218 3/ Dissect cells from the embryos as published elsewhere (Grant et al., 2013). A representative
- 219 example is shown in **Figure 2**. Briefly:
- 220 a. Transfer the selected embryos to a 60 mm Petri dish coated with 2% agarose and filled
 - 221 with 50% SS.
 - 222 b. Place the embryo of interest in a groove made in the agarose coating.
 - 223 c. Orient the embryo for easy handling of the cell of interest using a hair loop.
 - 224 d. Remove the vitelline membrane gently using sharp forceps. During this step, take care
 - 225 not to damage the embryo.
 - 226 e. Hold the embryo using sharp forceps on the opposite side of the cell of interest, and
 - 227 gently pull on either side to isolate the cell.
 - 228 f. Transfer isolated cells using a sterile Pasteur pipet into a micro-centrifuge tube.

229 **Protein Extraction and Enzymatic Digestion**

230 1/ Prepare consumables:

- 231 • Lysis buffer
- 232 • Acetone chilled to $-20\text{ }^{\circ}\text{C}$
- 233 • 50 mM ammonium bicarbonate
- 234 • 1 M dithiothreitol
- 235 • 1 M iodoacetamide
- 236 • Sonication bath (e.g., Brandson CPX 2800)

237 2/ Lyse the cells to release their content:

- 238 a. Remove the excess 50% SS from around the cell. Take care not to disrupt the cell.
- 239 b. Add 10 μL of lysis buffer (**Table 1**) and vortex for ~ 30 sec.
- 240 c. Sonicate for ~ 5 min, vortex for ~ 30 sec. Repeat this step 3 times.
- 241 d. (Optionally) Add protease inhibitor to the lysis buffer to minimize/avoid protein
- 242 degradation during this step.

243 3/ Reduce and alkylate protein cysteine bonds:

- 244 a. Add 0.5 μL of 1 M dithiothreitol to the sample, and incubate for 20–30 min at $60\text{ }^{\circ}\text{C}$.
- 245 b. Add 1 μL of 1 M iodoacetamide and incubate for 15 min in the dark at room temperature.
- 246 c. Quench the reaction by adding 0.5 μL of 1 M dithiothreitol.

247 4/ Purify proteins by cold acetone precipitation.

- 248 a. Add to the cell extract a volume of pure acetone that is 5 times that of the cell extract
- 249 ($\sim 50\text{ }\mu\text{L}$), and incubate at $-20\text{ }^{\circ}\text{C}$ overnight.
- 250 b. Recover the precipitated proteins by centrifugation at $10,000 \times g$ for 10 min and $4\text{ }^{\circ}\text{C}$.
- 251 c. Remove the supernatant.

- 252 d. Dry the pellet using a vacuum concentrator.
- 253 e. (Optional) Store the protein pellet at $-20\text{ }^{\circ}\text{C}$ or $-80\text{ }^{\circ}\text{C}$ for up to 3 months.
- 254 5/ Digest proteins for bottom-up proteomics analysis. A variety of enzymes or a combination
255 of enzymes can be used for this task (e.g., trypsin, lysine C). We choose trypsin due to its
256 benefits for MS analysis (Zhang et al., 2013).
- 257 a. Reconstitute the protein pellet in 50 mM ammonium bicarbonate.
- 258 b. Add $0.3\text{ }\mu\text{L}$ of $0.5\text{ }\mu\text{g}/\mu\text{L}$ trypsin (trypsin in 1 mM HCl), equivalent to a protease/protein
259 ratio of $\sim 1/50$.
- 260 c. Incubate overnight at $37\text{ }^{\circ}\text{C}$.
- 261 6/ (Optional) Store the digest at $-80\text{ }^{\circ}\text{C}$ for up to 3 months.

262 **Quantification**

263 The presented technology is compatible with well-established protocols in quantitative
264 proteomics. Stable isotope labeling with amino acids in cell culture (SILAC) allows barcoding of
265 proteins with isotopic labels for multiplexing quantification (Geiger et al., 2013). Label-free
266 quantification is an alternative strategy whereby peptide signal abundance is used as a proxy for
267 protein concentration. We have recently demonstrated label-free quantification (LFQ) for single
268 blastomeres of neural fates in the 16-cell embryo using the protocol presented here (Lombard-
269 Banek et al., 2016b). Alternatively, relative quantification can be performed using designer mass
270 tags. In this approach, proteins are digested to peptides and the peptides barcoded with isotopic
271 labels that can be distinguished by high-resolution MS. Multiple protocols allow for quantifying
272 protein expression at the level of peptides in high throughput via multiplexing, including tandem
273 mass tags (TMT) (Thompson et al., 2006; McAlister et al., 2014), and isobaric tag for relative
274 and absolute quantitation (iTRAQ) (Hunt et al., 2004), di-Leu (Xiang et al., 2010; Frost and Li,

275 2016). We have recently downscaled TMT-based multiplexed quantification to the protein
276 content of single blastomeres using the following strategy (adapted from the vendor), which we
277 then used to compare protein expression between the D11, V11, and V21 cells (Lombard-Banek
278 et al., 2016a) that are fated to give rise to different types of tissues (neural, epidermal, and
279 hindgut, respectively):

- 280 a. Add 15 μ L of TMT reagent to each digest and incubate for 1 h at room temperature.
- 281 b. Add 3.5 μ L of hydroxylamine and incubate for 15 min at room temperature.
- 282 c. Mix the samples together at a 1:1 ratio (volume or total protein content)
- 283 d. Dry the sample using a vacuum concentrator.
- 284 e. Add 5 μ L of 60% acetonitrile containing 0.05% formic acid.

285 **2. Sample Analysis using CE-ESI-MS**

286 Peptides are analyzed using a custom-built CE-ESI-MS platform (Nemes et al., 2013;
287 Onjiko et al., 2015b; Lombard-Banek et al., 2016a). Instructions regarding the construction and
288 operation of the platform are available from elsewhere (Nemes et al., 2013). Schematics of the
289 CE-ESI-MS instrument are shown in **Figure 3**. CE is selected to electrophoretically separate
290 peptides in a fused silica capillary by applying voltage difference across the capillary ends. As a
291 general rule, peptides with smaller size and higher charge state migrate faster through the
292 capillary. A high resolution mass spectrometer is used to sequence peptides via data-dependent
293 acquisition. In this approach, eluting peptides are detected based on single-stage (full) scans
294 (MS^1) and are sequenced by tandem-MS (MS^2 scans) using collision-induced dissociation (CID),
295 higher-energy collisional dissociation (HCD), or other fragmentation technologies. The tandem
296 mass spectra reveal sequence information for the peptides, as also exemplified for LGLGLELEA
297 in **Figure 4**. During quantification experiments, the TMT labels also dissociate from the peptide,

298 and the relative abundance of these TMT signals serves as quantitative measure of protein
299 abundance (**Figure 4C, right panel**).

300 **CE-ESI-MS Measurements**

301 1/ Build the CE-ESI-MS system as described elsewhere (Nemes et al., 2013; Onjiko et al.,
302 2015a). For bottom-up proteomics of single *Xenopus* blastomeres, operate the system as
303 recently established (Lombard-Banek et al., 2016a; Lombard-Banek et al., 2016b).

304 2/ Prepare the CE system ~15 min prior to start the experiments as follow:

- 305 a. Flush the capillary with background electrolyte solution (25% acetonitrile with 1 M
306 formic acid).
- 307 b. Flush the sheath capillary with electrospray solution (50% methanol with 0.1%
308 formic acid)
- 309 c. Turn on the electronics (high voltage power supplies, syringe pumps, mass
310 spectrometer, etc.) for ~30 min to stabilize operation.

311 3/ Inject the sample into the capillary as follows:

- 312 a. Transfer the capillary into the background electrolyte vial.
- 313 b. Deposit ~1 μ L of sample onto the sample microvial (see **Figure 3**).
- 314 c. Transfer the capillary from the BGE vial to the sample vial.
- 315 d. Elevate the injection stage by ~15 cm for ~3 min to syphon ~20 nL of the sample into
316 the CE capillary.
- 317 e. Lower the injection stage to level the capillary inlet to the outlet, and transfer the
318 capillary inlet end into the BGE vial.
- 319 f. Apply ~10,000 V to the background electrolyte vial to start electrophoretic separation
320 of the peptides.

- 321 g. Increase the electrospray voltage gradually until the cone jet mode is established for
322 efficient ionization (Nemes et al., 2007). Using a long-distance microscope, carefully
323 inspect the electrospray emitter to avoid electrical breakdown; electrical discharge,
324 spark, or arc risks the mass spectrometer. In our experiments, the electrospray emitter
325 is positioned ~0.5 cm from the mass spectrometer orifice and is biased to 3,000 V to
326 generate the cone-jet spray.
- 327 h. Ramp the separation voltage to ~18,000 V. In our system, we limit the separation
328 voltage to keep the CE current <8 μ A to prevent/minimize electrolysis or solvent
329 heating. Monitor the CE current and adjust the separation voltage as necessary. For
330 instructions on how to measure the current, refer to (Nemes et al., 2013).
- 331 i. Start MS acquisition with data-dependent acquisition as specified by the mass
332 spectrometer vendor. For example, we use the following settings for a quadrupole-
333 orbitrap linear ion trap mass spectrometer (Fusion, Thermo Scientific): MS¹
334 analyzer–resolution–scan range–injection time, orbitrap–60,000 FWHM– m/z 350-to-
335 1,600–100 ms; precursor ion selection window, 2 Da in the quadrupole cell;
336 fragmentation, HCD with 30% normalized energy in the multipole cell using nitrogen
337 collision gas; MS² analyzer–rate–maximum injection time, ion-trap–rapid scan–50
338 ms.

339 **Protein Identification**

340 Last, peptide sequences are compared to the proteome of the specimen (*Xenopus laevis*
341 here) to identify proteins. This step is facilitated by readily available proteomes from SwissProt,
342 UniProt, and experimentally determined RNA expression (Wang et al., 2012; Smits et al., 2014;
343 Wuhr et al., 2014). Well-established bioinformatics software packages are used to process raw

344 mass spectrometric data. For example, Proteome Discoverer (Thermo Scientific), ProteinScape
345 (Bruker Daltonics), and MaxQuant (Cox and Mann, 2008) interpret MS–tandem-MS datasets by
346 executing well-established search engines, such as SEQUEST (Eng et al., 1994), Mascot
347 (Perkins et al., 1999), and Andromeda (Cox et al., 2011)). The general strategy of bottom-up
348 proteomics has recently been reviewed in detail (Sadygov et al., 2004; Cox et al., 2011; Zhang et
349 al., 2013). We typically acquire tens of thousands to a million mass spectra, which identify
350 2,000–4,000 peptides in single blastomeres in the 16-cell embryo. These data allow us to identify
351 ~1,700 protein groups and quantify hundreds of proteins between the D11, V11, and V21 cells.

352 **3. Anticipated Results**

353 The CE-ESI-MS can be used to identify gene translational differences between cells. As
354 shown in **Figure 5**, we have used this approach to assess protein differences between
355 blastomeres of the 16-cell *Xenopus laevis* embryo (Lombard-Banek et al., 2016a; Lombard-
356 Banek et al., 2016b). Cell types with different tissue developmental fates were analyzed: the
357 midline dorsal-animal cell (named D11) develops mainly into the retina and brain, the midline
358 ventral-animal cell (named V11) gives rise primarily to the head and trunk epidermis, and the
359 midline ventral-vegetal cell (named V21) is the primary precursor of the hindgut. The approach
360 allowed the identification of 1,709 protein groups (<1% false discovery rate, FDR) from ~20 ng
361 of protein digest, corresponding to ~0.2% of the total protein content of the blastomere
362 (Lombard-Banek et al., 2016a). Many of the identified proteins are known to be involved in
363 different cell fates. For example, Geminin (Gem) and Isthmin (Ism) were detected in the D11
364 cells in our measurements, and these proteins are involved in brain development (Pera et al.,
365 2002; Seo et al., 2005), which is the stereotypical fate of D11 cells (Moody, 1987a). Multiplexed
366 quantification by TMTs provided comparative evaluation for 152 non-redundant protein groups

367 between the cell types (**Figure 5B, left**), including many that were significantly differentially
368 expressed based between the cell types ($p < 0.05$, fold change ≥ 1.3). We have also performed
369 label free quantitation (LFQ) to compare D11 cells that were isolated at similar developmental
370 phase of the 16-cell *Xenopus laevis* embryos (**Figure 5A**). A Pearson correlation analysis
371 showed similar expression levels for the majority of proteins between the D11 cells (see proteins
372 along linear fits). The study also found 25 proteins that were differentially accumulated in the
373 respective cells, suggesting highly variable expression (**Figure 5B, right**) (Lombard-Banek et
374 al., 2016b). These data on translational cell heterogeneity complement transcriptomic
375 information on cell differences (Flachsova et al., 2013), but also provide new insights into how
376 differential gene expression sets up different cell fates and the major developmental axes of the
377 early embryo.

378 **Conclusions**

379 High-sensitivity MS enables the identification and quantification of a sufficiently large number
380 of proteins to study cell and developmental processes at the level of individual cells. Advances in
381 sampling (smaller single cells), protein processing, microanalytical MS, and bioinformatics have
382 enabled the discovery characterization of hundreds to thousands of proteins in single cells.
383 Unbiased measurement of protein translation by MS complements genomic and transcriptomic
384 information, essentially laying down the foundation of the molecular characterization of cell
385 heterogeneity. Knowledge of genomic, transcriptomic, proteomic, and metabolomic processes
386 paves the way to understanding how differential gene expression establishes cell heterogeneity
387 for normal development and disease states.
388

389 **Authors and Contributors**

390 C.L., S.A.M., and P.N. wrote the manuscript.

391

392 **Funding**

393 This research was supported by National Science Foundation Grant DBI-1455474 (to P.N. and
394 S.A.M.) and the George Washington University Start-Up Funds (to P.N.) and Columbian
395 College Facilitating Funds (to P.N. and S.A.M.). The content of the presented work was solely
396 the responsibility of the authors and does not necessarily represent the official views of the
397 funding agencies.

398

399 **References**

- 400 Abrams, E.W., and Mullins, M.C. (2009). Early zebrafish development: It's in the maternal
401 genes. *Curr. Opin. Genet. Dev.* 19(4), 396-403. doi: 10.1016/j.gde.2009.06.002.
- 402 Aebersold, R., and Mann, M. (2003). Mass spectrometry-based proteomics. *Nature* 422(6928),
403 198-207. doi: 10.1038/nature01511.
- 404 Altschuler, S.J., and Wu, L.F. (2010). Cellular heterogeneity: Do differences make a difference?
405 *Cell* 141(4), 559-563. doi: 10.1016/j.cell.2010.04.033.
- 406 Bendall, S.C., Simonds, E.F., Qiu, P., Amir, E.A.D., Krutzik, P.O., Finck, R., et al. (2011).
407 Single-cell mass cytometry of differential immune and drug responses across a human
408 hematopoietic continuum. *Science* 332(6030), 687-696. doi: 10.1126/science.1198704.
- 409 Cox, J., and Mann, M. (2008). MaxQuant enables high peptide identification rates,
410 individualized p.p.b.-range mass accuracies and proteome-wide protein quantification.
411 *Nat. Biotechnol.* 26(12), 1367-1372. doi: 10.1038/nbt.1511.
- 412 Cox, J., Neuhauser, N., Michalski, A., Scheltema, R.A., Olsen, J.V., and Mann, M. (2011).
413 Andromeda: A peptide search engine integrated into the MaxQuant environment. *J.*
414 *Proteome Res.* 10(4), 1794-1805. doi: 10.1021/pr101065j.
- 415 Cuykendall, T.N., and Houston, D.W. (2010). Identification of germ plasm-associated transcripts
416 by microarray analysis of *Xenopus* vegetal cortex RNA. *Dev. Dyn.* 239(6), 1838-1848.
417 doi: 10.1002/dvdy.22304.
- 418 Davidson, E.H. (1990). How embryos work: A comparative view of diverse modes of cell fate
419 specification. *Development* 108(3), 365-389.
- 420 De Domenico, E., Owens, N.D.L., Grant, I.M., Gomes-Faria, R., and Gilchrist, M.J. (2015).
421 Molecular asymmetry in the 8-cell stage *Xenopus tropicalis* embryo described by single

422 blastomere transcript sequencing. *Dev. Biol.* 408(2), 252-268. doi:
423 10.1016/j.ydbio.2015.06.010.

424 Eng, J.K., McCormack, A.L., and Yates, J.R. (1994). An approach to correlate tandem mass-
425 spectral data of peptides with amino-acids sequences in a protein database. *J. Am. Soc.*
426 *Mass Spectrom.* 5(11), 976-989. doi: 10.1016/1044-0305(94)80016-2.

427 Flachsova, M., Sindelka, R., and Kubista, M. (2013). Single blastomere expression profiling of
428 *Xenopus laevis* embryos of 8 to 32-cells reveals developmental asymmetry. *Sci. Rep.* 3.
429 doi: 10.1038/srep02278.

430 Frost, D.C., and Li, L.J. (2016). "High-throughput quantitative proteomics enabled by mass
431 defect-based 12-plex diLeu isobaric tags," in *Quantitative Proteomics by Mass*
432 *Spectrometry, 2nd Edition*, ed. S. Sechi. (Totowa: Humana Press Inc), 169-194.

433 Gajecka, M. (2016). Unrevealed mosaicism in the next-generation sequencing era. *Mol. Genet.*
434 *Genomics* 291(2), 513-530. doi: 10.1007/s00438-015-1130-7.

435 Gallagher, B.C., Hainski, A.M., and Moody, S.A. (1991). Autonomous differentiation of dorsal
436 axial structures from an animal cap cleavage stage blastomere in *Xenopus*. *Development*
437 112(4), 1103-1114.

438 Gaur, S., Mandelbaum, M., Herold, M., Majumdar, H.D., Neilson, K.M., Maynard, T.M., et al.
439 (2016). Neural transcription factors bias cleavage stage blastomeres to give rise to neural
440 ectoderm. *The Journal of Genetics and Development* 54, 334-349.

441 Geiger, T., Velic, A., Macek, B., Lundberg, E., Kampf, C., Nagaraj, N., et al. (2013). Initial
442 quantitative proteomic map of 28 mouse tissues using the SILAC mouse. *Mol. Cell.*
443 *Proteomics* 12(6), 1709-1722. doi: 10.1074/mcp.M112.024919.

444 Giesen, C., Wang, H.A.O., Schapiro, D., Zivanovic, N., Jacobs, A., Hattendorf, B., et al. (2014).
445 Highly multiplexed imaging of tumor tissues with subcellular resolution by mass
446 cytometry. *Nat. Methods* 11(4), 417-422. doi: 10.1038/nmeth.2869.

447 Grant, P.A., Herold, M.B., and Moody, S.A. (2013). Blastomere explants to test for cell fate
448 commitment during embryonic development. *J. Vis. Exp.* (71). doi: 10.3791/4458.

449 Grant, P.A., Yan, B., Johnson, M.A., Johnson, D.L.E., and Moody, S.A. (2014). Novel animal
450 pole-enriched maternal mRNAs are preferentially expressed in neural ectoderm. *Dev.*
451 *Dyn.* 243(3), 478-496. doi: Doi 10.1002/Dvdy.24082.

452 Guerrero, I.C., and Kleiner, O. (2005). Application of mass spectrometry in proteomics. *Biosci.*
453 *Rep.* 25(1-2), 71-93. doi: 10.1007/s10540-005-2849-x.

454 Hainski, A.M., and Moody, S.A. (1992). *Xenopus* maternal Rnas from a dorsal animal
455 blastomere induce a secondary axis in host embryos. *Development* 116(2), 347-&.

456 Haston, K.M., and Reijo-Pera, R.A. (2007). "Germ line determinants and oogenesis. ," in
457 *Principles of Developmental Genetics*, ed. S.A. Moody. Academic Press, NY), 150-172.

458 Heasman, J. (2006a). Maternal determinants of embryonic cell fate. *Semin. Cell. Dev. Biol.*
459 17(1), 93-98. doi: 10.1016/j.semcdb.2005.11.005.

460 Heasman, J. (2006b). Patterning the early *Xenopus* embryo. *Development* 133(7), 1205-1217.
461 doi: 10.1242/dev.02304.

462 Hebert, A.S., Richards, A.L., Bailey, D.J., Ulbrich, A., Coughlin, E.E., Westphall, M.S., et al.
463 (2014). The one hour yeast proteome. *Mol. Cell. Proteomics* 13(1), 339-347. doi: DOI
464 10.1074/mcp.M113.034769.

465 Hofstadler, S.A., Swanek, F.D., Gale, D.C., Ewing, A.G., and Smith, R.D. (1995). Capillary
466 electrophoresis electrospray ionization Fourier transform ion cyclotron resonance mass

467 spectrometry for direct analysis of cellular proteins. *Anal. Chem.* 67(8), 1477-1480. doi:
468 10.1021/ac00104a028.

469 Hunt, T., Huang, Y., Ross, P., Pillai, S., Purkayastha, S., and Pappin, D. (2004). Protein
470 expression analysis and biomarker identification and quantification using multiplexed
471 isobaric tagging technology - iTRAQ reagents. *Mol. Cell. Proteomics* 3(10), S286-S286.

472 Jacobs, K., Mertzaniidou, A., Geens, M., Nguyen, H.T., Staessen, C., and Spits, C. (2014). Low-
473 grade chromosomal mosaicism in human somatic and embryonic stem cell populations.
474 *Nat. Commun.* 5, 4227-4237. doi: 10.1038/ncomms5227.

475 Junker, J.P., and van Oudenaarden, A. (2015). Single-cell transcriptomics enters the age of mass
476 production. *Mol. Cell* 58(4), 563-564. doi: 10.1016/j.molcel.2015.05.019.

477 Kanter, I., and Kalisky, T. (2015). Single cell transcriptics: methods and applications. *Front.*
478 *Oncol.* 5. doi: 10.3389/fonc.2015.00053.

479 Kenyon, K.L. (2007). "Patterning the anterior-posterior axis during *Drosophila* embryogenesis,"
480 in *Principles of Developmental Genetics*, ed. S.A. Moody. Academic Press, NY), 173-
481 200.

482 King, M.L., Messitt, T.J., and Mowry, K.L. (2005). Putting RNAs in the right place at the right
483 time: RNA localization in the frog oocyte. *Biol. Cell* 97(1), 19-33.

484 Kolisko, M., Boscaro, V., Burki, F., Lynn, D.H., and Keeling, P.J. (2014). Single-cell
485 transcriptomics for microbial eukaryotes. *Curr. Biol.* 24(22), R1081-R1082. doi:
486 10.1016/j.cub.2014.10.026.

487 Kuster, B. (2014). Mass spectrometry based draft of the human proteome. *Mol. Cell. Proteomics*
488 13(8), S15-S15.

489 Lee, H.S., Sokol, S.Y., Moody, S.A., and Daar, I.O. (2012). *Using 32-cell stage *Xenopus**
490 *embryos to probe PCP signaling*. Springer New York.

491 Li, S.Y., Plouffe, B.D., Belov, A.M., Ray, S., Wang, X.Z., Murthy, S.K., et al. (2015). An
492 integrated platform for isolation, processing, and mass spectrometry-based proteomic
493 profiling of rare cells in whole blood. *Mol. Cell. Proteomics* 14(6), 1672-1683. doi:
494 10.1074/mcp.M114.045724.

495 Liang, Q., Conte, N., Skarnes, W.C., and Bradley, A. (2008). Extensive genomic copy number
496 variation in embryonic stem cells. *Proc. Natl. Acad. Sci. U. S. A.* 105(45), 17453-17456.
497 doi: 10.1073/pnas.0805638105.

498 Lindeman, R.E., and Pelegri, F. (2010). Vertebrate maternal-effect genes: Insights into
499 fertilization, early cleavage divisions, and germ cell determinant localization from studies
500 in the zebrafish. *Mol. Reprod. Dev.* 77(4), 299-313. doi: 10.1002/mrd.21128.

501 Lombard-Banek, C., Moody, S.A., and Nemes, P. (2016a). Single-cell mass spectrometry for
502 discovery proteomics: Quantifying translational cell heterogeneity in the 16-cell frog
503 (*Xenopus*) embryo. *Angew. Chem. Int. Edit.* 55(7), 2454-2458. doi:
504 10.1002/anie.201510411.

505 Lombard-Banek, C., Reddy, S., Moody, S.A., and Nemes, P. (2016b). Label-free quantification
506 of proteins in single embryonic cells with neural fate in the cleavage-stage frog (*Xenopus*
507 *laevis*) embryo using CE-ESI-HRMS. *Submitted*.

508 McAlister, G.C., Nusinow, D.P., Jedrychowski, M.P., Wuhr, M., Huttlin, E.L., Erickson, B.K., et
509 al. (2014). MultiNotch MS³ enables accurate, sensitive, and multiplexed detection of
510 differential expression across cancer cell line proteomes. *Anal. Chem.* 86(14), 7150-7158.
511 doi: 10.1021/ac502040v.

512 McConnell, M.J., Lindberg, M.R., Brennand, K.J., Piper, J.C., Voet, T., Cowing-Zitron, C., et al.
513 (2013). Mosaic copy number variation in human neurons. *Science* 342(6158), 632-637.
514 doi: 10.1126/science.1243472.

515 Mellors, J.S., Jorabchi, K., Smith, L.M., and Ramsey, J.M. (2010). Integrated microfluidic
516 device for automated single cell analysis using electrophoretic separation and
517 electrospray ionization mass spectrometry. *Anal. Chem.* 82(3), 967-973. doi:
518 10.1021/ac902218y.

519 Mitra, A.K., Stessman, H., Linden, M.A., and Van Ness, B. (2014). Single-cell transcriptomics
520 identifies intra-tumor heterogeneity in Human myeloma cell lines. *Blood* 124(21).

521 Moody, S.A. (1987a). Fates of the blastomeres of the 16-cell stage *Xenopus* embryo. *Dev. Biol.*
522 119(2), 560-578.

523 Moody, S.A. (1987b). Fates of the blastomeres of the 32-cell-stage *Xenopus* embryo. *Dev. Biol.*
524 122(2), 300-319.

525 Moody, S.A. (2012). *Testing retina fate commitment in Xenopus by blastomere deletion,*
526 *transplantation, and explant culture.* Springer New York.

527 Moody, S.A., and Kline, M.J. (1990). Segregation of fate during cleavage of frog (*Xenopus*
528 *laevis*) blastomeres. *Anat. Embryol.* 182(4), 347-362. doi: 10.1007/bf02433495.

529 Nemes, P., Marginean, I., and Vertes, A. (2007). Spraying mode effect on droplet formation and
530 ion chemistry in electrosprays. *Anal. Chem.* 79(8), 3105-3116. doi: Doi
531 10.1021/Ac062382i.

532 Nemes, P., Rubakhin, S.S., Aerts, J.T., and Sweedler, J.V. (2013). Qualitative and quantitative
533 metabolomic investigation of single neurons by capillary electrophoresis electrospray
534 ionization mass spectrometry. *Nat. Protoc.* 8(4), 783-799. doi: DOI
535 10.1038/nprot.2013.035.

536 Onjiko, R.M., Moody, S.A., and Nemes, P. (2015a). Single-cell mass spectrometry reveals small
537 molecules that affect cell fates in the 16-cell embryo. *Proceedings of the National*
538 *Academy of Sciences of the United States of America* 112(21), 6545-6550. doi:
539 10.1073/pnas.1423682112.

540 Onjiko, R.M., Moody, S.A., and Nemes, P. (2015b). Single-cell mass spectrometry reveals small
541 molecules that affect cell fates in the 16-cell embryo. *Proc. Natl. Acad. Sci. U. S. A.*
542 112(21), 6545-6550. doi: 10.1073/pnas.1423682112.

543 Onjiko, R.M., Morris, S.E., Moody, S.A., and Nemes, P. (2016). Single-cell mass spectrometry
544 with multi-solvent extraction identifies metabolic differences between left and right
545 blastomeres in the 8-cell frog (*Xenopus*) embryo. *Analyst.* doi: 10.1039/c6an00200e.

546 Passarelli, M.K., and Ewing, A.G. (2013). Single-cell imaging mass spectrometry. *Curr. Opin.*
547 *Chem. Biol.* 17(5), 854-859. doi: 10.1016/j.cbpa.2013.07.017.

548 Pera, E.M., Kim, J.I., Martinez, S.L., Brechner, M., Li, S.Y., Wessely, O., et al. (2002). Isthmin
549 is a novel secreted protein expressed as part of the Fgf-8 synexpression group in the
550 *Xenopus* midbrain-hindbrain organizer. *Mech. Dev.* 116(1-2), 169-172.

551 Perkins, D.N., Pappin, D.J.C., Creasy, D.M., and Cottrell, J.S. (1999). Probability-based protein
552 identification by searching sequence databases using mass spectrometry data.
553 *Electrophoresis* 20(18), 3551-3567. doi: 10.1002/(sici)1522-
554 2683(19991201)20:18<3551::aid-elps3551>3.0.co;2-2.

555 Peshkin, L., Wuhr, M., Pearl, E., Haas, W., Freeman, R.M., Gerhart, J.C., et al. (2015). On the
556 relationship of protein and mRNA dynamics in vertebrate embryonic development. *Dev.*
557 *Cell* 35(3), 383-394. doi: 10.1016/j.devcel.2015.10.010.

558 Radford, H.E., Meijer, H.A., and de Moor, C.H. (2008). Translational control by cytoplasmic
559 polyadenylation in *Xenopus* oocytes. *BBA-Gene Regul. Mech.* 1779(4), 217-229. doi:
560 10.1016/j.bbagr.2008.02.002.

561 Raj, A., and van Oudenaarden, A. (2008). Nature, nurture, or chance: Stochastic gene expression
562 and its consequences. *Cell* 135(2), 216-226. doi: 10.1016/j.cell.2008.09.050.

563 Ratnaparkhi, G.S., and Courey, A.J. (2007). "Signaling cascades, gradients, and gene networks
564 in dorsal/ventral patterning.," in *Principles of Developmental Genetics*, ed. E.S.A.
565 Moody. Academic Press, NY), 216-240.

566 Rubakhin, S.S., Romanova, E.V., Nemes, P., and Sweedler, J.V. (2011). Profiling metabolites
567 and peptides in single cells. *Nat. Methods* 8(4), S20-S29. doi: 10.1038/nmeth.1549.

568 Sadygov, R.G., Cociorva, D., and Yates, J.R. (2004). Large-scale database searching using
569 tandem mass spectra: Looking up the answer in the back of the book. *Nat. Methods* 1(3),
570 195-202. doi: 10.1038/nmeth725.

571 Seo, S., Herr, A., Lim, J.W., Richardson, G.A., Richardson, H., and Kroll, K.L. (2005). Geminin
572 regulates neuronal differentiation by antagonizing Brg1 activity. *Genes Dev.* 19(14),
573 1723-1734. doi: 10.1101/gad.1319105.

574 Shrestha, B., Sripadi, P., Reschke, B.R., Henderson, H.D., Powell, M.J., Moody, S.A., et al.
575 (2014). Subcellular metabolite and lipid analysis of *Xenopus laevis* eggs by LAESI mass
576 spectrometry. *PLoS One* 9(12). doi: 10.1371/journal.pone.0115173.

577 Sindelka, R., Sidova, M., Svec, D., and Kubista, M. (2010). Spatial expression profiles in the
578 *Xenopus laevis* oocytes measured with qPCR tomography. *Methods* 51(1), 87-91. doi:
579 10.1016/j.ymeth.2009.12.011.

580 Singh, D.K., Ku, C.J., Wichaidit, C., Steininger, R.J., Wu, L.F., and Altschuler, S.J. (2010).
581 Patterns of basal signaling heterogeneity can distinguish cellular populations with
582 different drug sensitivities. *Mol. Syst. Biol.* 6, 369. doi: 10.1038/msb.2010.22.

583 Smits, A.H., Lindeboom, R.G.H., Perino, M., van Heeringen, S.J., Veenstra, G.J.C., and
584 Vermeulen, M. (2014). Global absolute quantification reveals tight regulation of protein
585 expression in single *Xenopus* eggs. *Nucleic Acids Res.* 42(15), 9880-9891. doi: Doi
586 10.1093/Nar/Gku661.

587 Sullivan, S.A., Akers, L., and Moody, S.A. (2001). foxD5a, a *Xenopus* winged helix gene,
588 maintains an immature neural ectoderm via transcriptional repression that is dependent
589 on the C-terminal domain. *Dev. Biol.* 232(2), 439-457. doi: DOI 10.1006/dbio.2001.0191.

590 Sun, L.L., Bertke, M.M., Champion, M.M., Zhu, G.J., Huber, P.W., and Dovichi, N.J. (2014).
591 Quantitative proteomics of *Xenopus laevis* embryos: expression kinetics of nearly 4000
592 proteins during early development. *Sci. Rep.* 4. doi: 10.1038/srep04365.

593 Thompson, A., Schaefer, J., Kuhn, K., Kienle, S., Schwarz, J., Schmidt, G., et al. (2006).
594 Tandem mass tags: A novel quantification strategy for comparative analysis of complex
595 protein mixtures by MS/MS *Anal. Chem.* 78(12), 4235-4235. doi: 10.1021/ac060310l.

596 Valaskovic, G.A., Kelleher, N.L., and McLafferty, F.W. (1996). Attomole protein
597 characterization by capillary electrophoresis mass spectrometry. *Science* 273(5279),
598 1199-1202. doi: 10.1126/science.273.5279.1199.

599 Vastag, L., Jorgensen, P., Peshkin, L., Wei, R., Rabinowitz, J.D., and Kirschner, M.W. (2011).
600 Remodeling of the metabolome during early frog development. *PLoS One* 6(2), e16881.
601 doi: 10.1371/journal.pone.0016881.

602 Vijg, J. (2014). Somatic mutations, genome mosaicism, cancer and aging. *Curr. Opin. Genet.*
603 *Dev.* 26, 141-149. doi: 10.1016/j.gde.2014.04.002.

604 Vogel, C., and Marcotte, E.M. (2012). Insights into the regulation of protein abundance from
605 proteomic and transcriptomic analyses. *Nat. Rev. Genet.* 13(4), 227-232. doi:
606 10.1038/nrg3185.

607 Walther, T.C., and Mann, M. (2010). Mass spectrometry-based proteomics in cell biology. *J.*
608 *Cell Biol.* 190(4), 491-500. doi: 10.1083/jcb.201004052.

609 Wang, X.J., Slebos, R.J.C., Wang, D., Halvey, P.J., Tabb, D.L., Liebler, D.C., et al. (2012).
610 Protein identification using customized protein sequence databases derived from RNA-
611 seq data. *J. Proteome Res.* 11(2), 1009-1017. doi: 10.1021/pr200766z.

612 White, J.A., and Heasman, J. (2008). Maternal control of pattern formation in *Xenopus laevis*. *J*
613 *Exp. Zool. Part B* 310B(1), 73-84. doi: 10.1002/jez.b.21153.

614 Wilhelm, M., Schlegl, J., Hahne, H., Gholami, A.M., Lieberenz, M., Savitski, M.M., et al.
615 (2014). Mass-spectrometry-based draft of the human proteome. *Nature* 509(7502), 582-
616 587. doi: 10.1038/nature13319.

617 Wuhr, M., Freeman, R.M., Jr., Presler, M., Horb, M.E., Peshkin, L., Gygi, S.P., et al. (2014).
618 Deep proteomics of the *Xenopus laevis* egg using an mRNA-derived reference database.
619 *Curr. Biol.* 24(13), 1467-1475. doi: 10.1016/j.cub.2014.05.044.

620 Wuhr, M., Guttler, T., Peshkin, L., McAlister, G.C., Sonnett, M., Ishihara, K., et al. (2015). The
621 nuclear proteome of a vertebrate. *Curr. Biol.* 25(20), 2663-2671. doi:
622 10.1016/j.cub.2015.08.047.

623 Xanthos, J.B., Kofron, M., Wylie, C., and Heasman, J. (2001). Maternal VegT is the initiator of a
624 molecular network specifying endoderm in *Xenopus laevis*. *Development* 128(2), 167-
625 180.

626 Xiang, F., Ye, H., Chen, R.B., Fu, Q., and Li, L.J. (2010). N,N-dimethyl leucines as novel
627 isobaric tandem mass tags for quantitative proteomics and peptidomics. *Anal. Chem.*
628 82(7), 2817-2825. doi: 10.1021/ac902778d.

629 Yan, B., and Moody, S.A. (2007). The competence of *Xenopus* blastomeres to produce neural
630 and retinal progeny is repressed by two endo-mesoderm promoting pathways. *Dev. Biol.*
631 305(1), 103-119. doi: DOI 10.1016/j.ydbio.2007.01.040.

632 Zenobi, R. (2013). Single-cell metabolomics: analytical and biological perspectives. *Science*
633 342(6163), 1201. doi: 10.1126/science.1243259.

634 Zhang, Y.Y., Fonslow, B.R., Shan, B., Baek, M.C., and Yates, J.R. (2013). Protein analysis by
635 shotgun/bottom-up proteomics. *Chem. Rev.* 113(4), 2343-2394. doi: 10.1021/cr3003533.

636
637

638 **Tables**639 **Table 1.** Solutions and their uses.

| Solution /buffer | Composition | Usage | Storage conditions |
|------------------------------|---|---|---------------------------|
| Cysteine Hydrochloride | 2% (w/v) cysteine hydrochloride, pH 8 adjusted with 10 N NaOH drop wise | Removes the jelly coats surrounding embryos | Make fresh |
| Steinberg's Solution (SS) | 60 mM NaCl, 0.67 mM KCl, 0.83 mM MgSO ₄ , 0.34 mM Ca(NO ₃) ₂ , 4 mM Tris-HCl, 0.66 mM Tris base, in distilled water, pH 7.4. Autoclaved. Store in incubator for months. | Provides media for culturing embryos | 4–14 °C |
| Lysis Buffer | 1% sodium dodecyl sulfate (SDS), 150 mM NaCl, 20 mM Tris-HCl pH 8, 5 mM EDTA in distilled water | Lyses cells/tissues | 4 °C |
| Sample Solvent | 50–60% acetonitrile in water, 0.05% acetic acid (all solvents are LC-MS grade) | Reconstitutes protein digest | 4 °C |
| Background Electrolyte (BGE) | 25% acetonitrile in water, 1 M formic acid (all solvents are LC-MS grade) | Electrolyte for CE | 4 °C |
| Electrospray Sheath Liquid | 50% methanol in water, 0.1% formic acid (all solvents are LC-MS grade) | Stabilizes ESI-MS operation | 4 °C |

640

Provisional

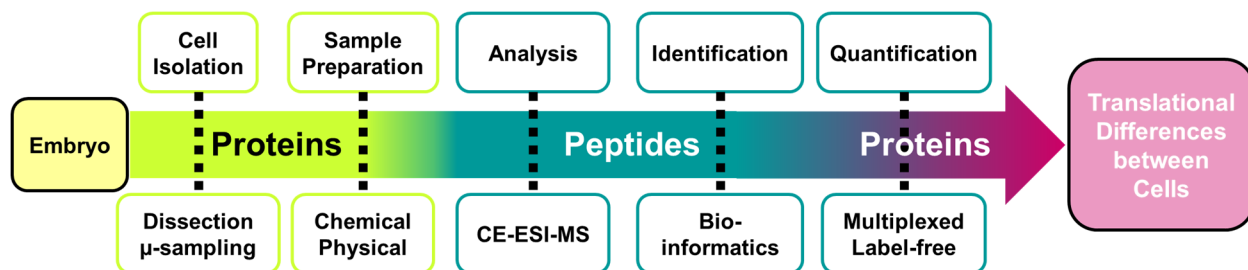
641 **Table 2.** Troubleshooting advice for CE-ESI-MS for bottom-up proteomics.

| Issues | Potential Causes | Advice |
|---------------------------------------|---|---|
| No peptides detected | Failed enzymatic digestion | Repeat analysis; if problem persists, repeat protein digestion (use standard proteins as quality control) |
| CE current drops drastically | Capillary is clogged or a bubble was injected | Flush the capillary with the BGE for ~10–15 min; repeat analysis |
| Electrospray is unstable | Electrolysis in the CE-ESI interface; the sheath flow connection is loose | Lower the spray voltage; revise connections; repeat analysis |
| Low number of protein identifications | Erroneous injection; inaccurate calibration of the mass spectrometer | Repeat analysis; calibrate the mass spectrometer |

642

Provisional

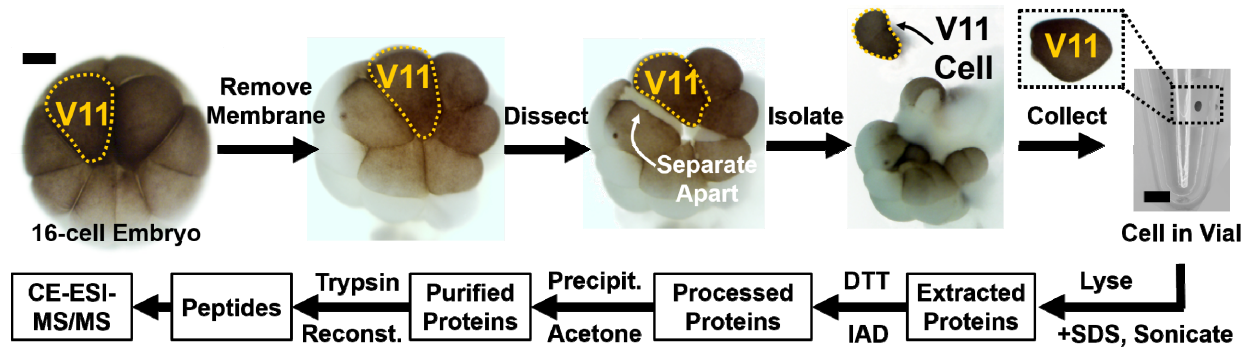
643 **FIGURES**



644

645 **Figure 1.** Analytical workflow for the bottom-up measurements of protein expression in single
646 embryonic cells. A custom-built high-sensitivity capillary electrophoresis electrospray ionization
647 mass spectrometer (CE-ESI-MS) is used to identify and quantify proteins.

Provisional



648

649

650

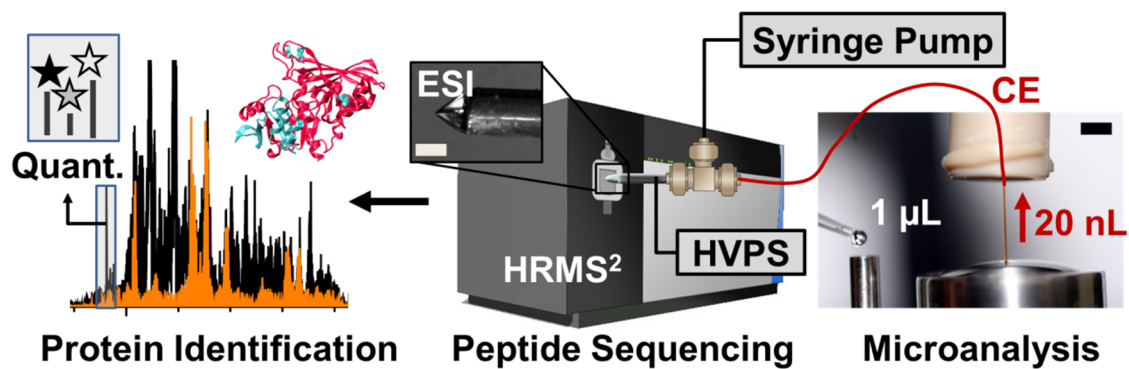
651

652

653

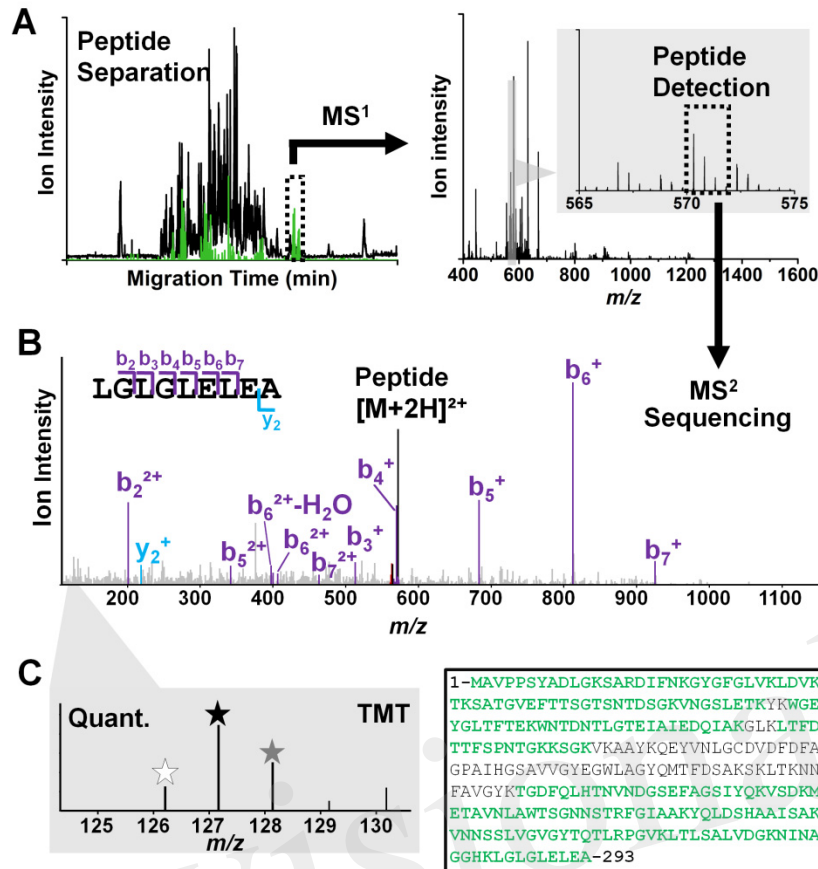
654

Figure 2. Isolation of identified cells and processing of their protein content. Example shows how the epidermal-fated ventral-animal cell (named V11) was identified in the 16-cell *Xenopus laevis* embryo based on pigmentation, cell size, and location in reference to established cell fate maps (Moody, 1987b; a). The cell was processed via bottom-up proteomic workflow, and the resulting peptides collected for proteomic analysis. Key: DTT, dithiothreitol; IAD, iodoacetamide. Scale bar = 200 μm (embryo), 1.25 mm (vial).



655
 656 **Figure 3.** Schematics of the high-sensitivity proteomic analyzer. The platform integrates
 657 microanalytical capillary electrophoresis (CE), electrospray ionization (ESI), and high-resolution
 658 tandem mass spectrometry (HRMS²). Scale bar = 150 µm (ESI), 1.5 mm (CE panel). (Figure
 659 adapted with permission from Ref. (Lombard-Banek et al., 2016a))

Provisional



Vdac2: 90% Sequence Coverage

660

661 **Figure 4.** Peptide identification/quantification in CE-ESI-HRMS² using a bottom-up strategy.

662 **(A)** Peptides are electrophoretically separated (**left panel**) and their accurate mass is measured

663 **(right panel).** **(B)** Peptide signals are sequenced by tandem MS (MS²). For example, a signal

664 was detected with m/z 572.33 at ~50 min separation, which was assigned to the sequence

665 LGLGLELEA based on the MS² data. **(C)** Peptides are quantified and assigned to the source

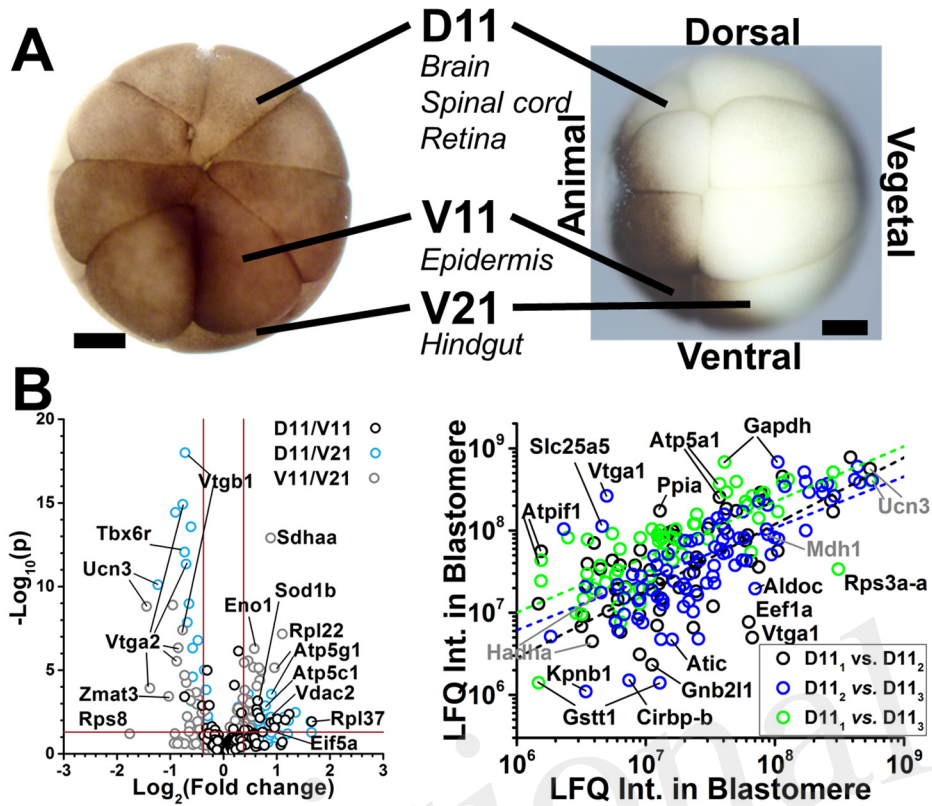
666 protein. Tandem mass tags (TMT) with different m/z values are used to barcode peptides from

667 different cells, allowing their simultaneous analysis (multiplexing) with higher throughput (**left**

668 **panel**). For example, the sequence LGLGLELEA was unique to the voltage-dependent anion

669 channel 2 protein in the *Xenopus* proteome. The presence of other peptides allowed identifying

670 this protein in high sequence coverage; see detected sequence in green (**right panel**).



671

672 **Figure 5.** Examples of protein identification–quantification between single embryonic cells. (A)

673 The D11, V11, and V21 cells have different tissues fates in the frog *Xenopus laevis*. Scale bars:

674 250 μm . (Figure reprinted with permission from (Onjiko et al., 2015b)). (B) These cells were

675 dissected from different 16-cell *Xenopus laevis* embryos and analyzed using multiplexed (left

676 panel) and label-free quantification (right panel). Volcano plots reveal gene translation

677 differences between the V11, D11, and V21 cell types (left). Pearson correlation analysis of

678 protein expression finds similar protein expression for the majority of proteins between D11

679 blastomeres, and detectable differences for others (right panel). (Figures adapted with

680 permission from (Lombard-Banek et al., 2016a; Lombard-Banek et al., 2016b)).

Figure 01.TIF

Provisional

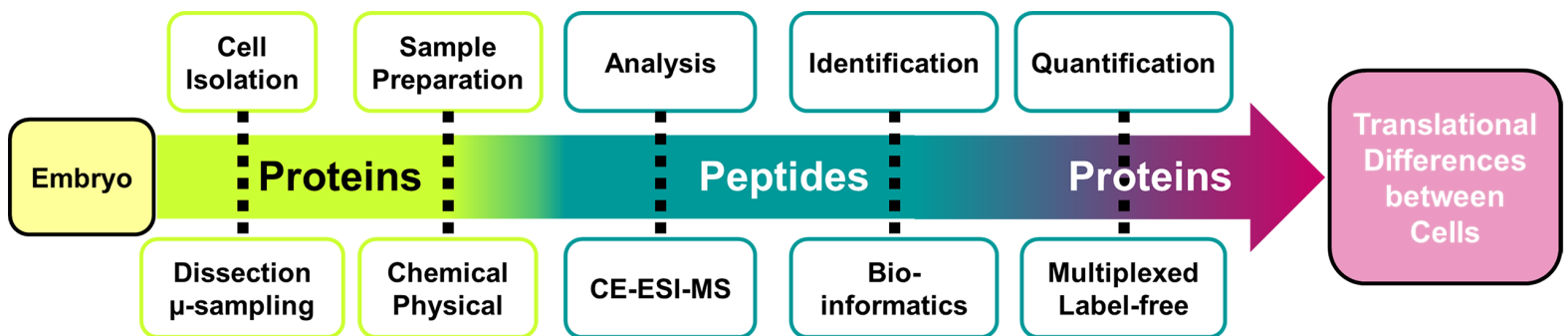
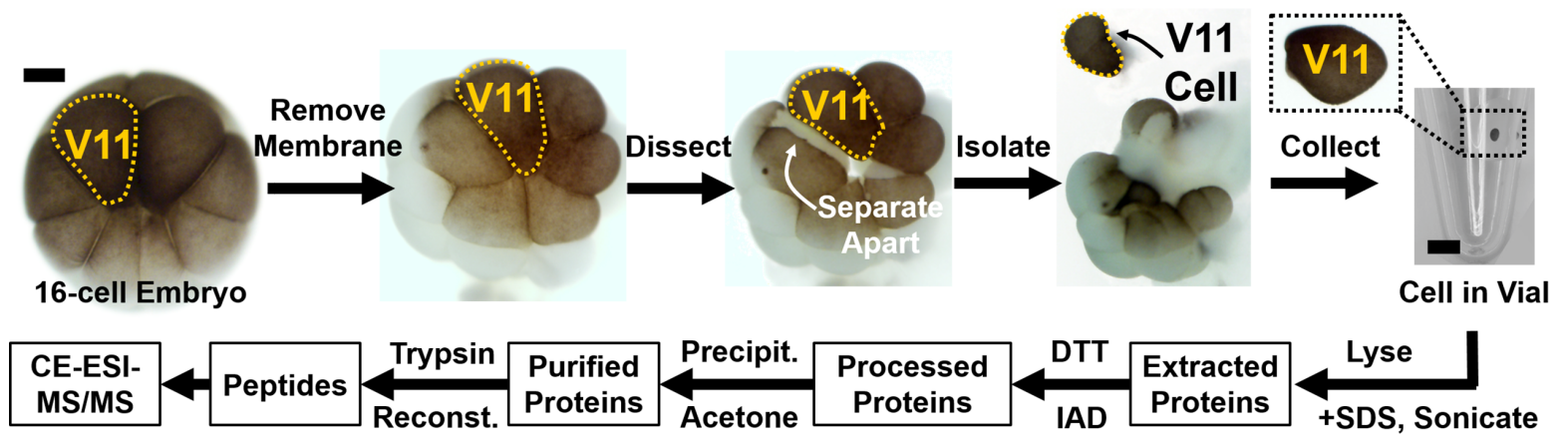


Figure 02.TIF

Provisional



Provisional

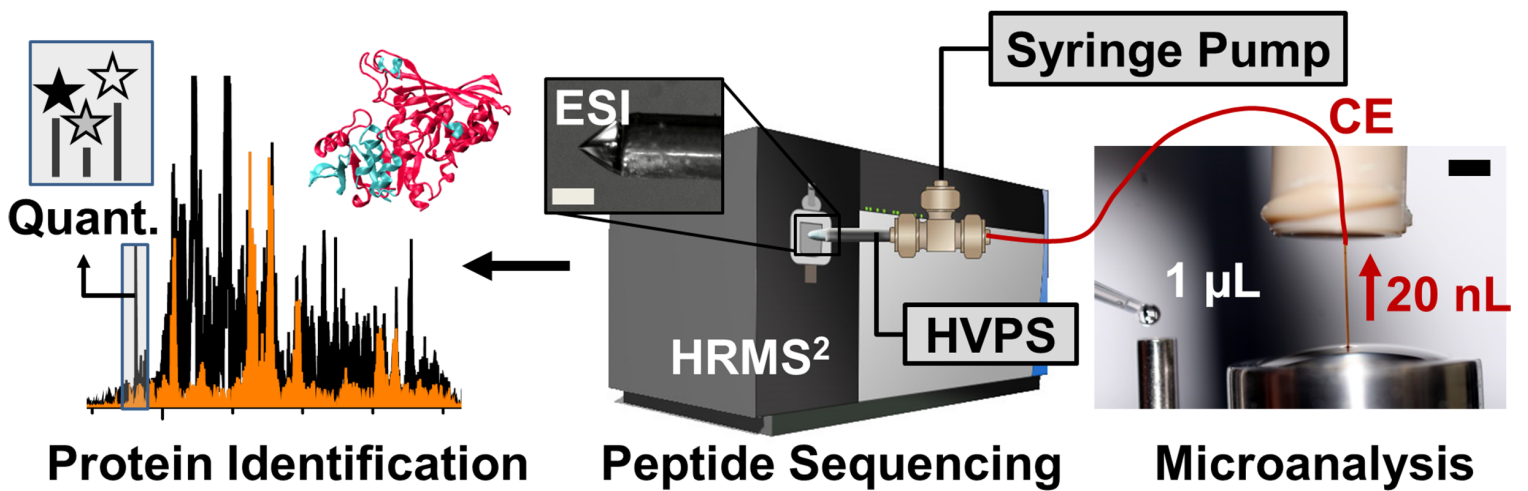


Figure 04.TIF

